Instability of hot electroweak theory: Bounds on m_H and m_t

Peter Arnold and Stamatis Vokos
High Energy Physics Division, Argonne National Laboratory, Argonne, Illinois 60439
(Received 17 June 1991)

The electroweak vacuum need not be absolutely stable. For certain top-quark and Higgs-boson masses in the minimal standard model, it is instead metastable with a lifetime exceeding the present age of the Universe. The decay of our vacuum may be nucleated at low temperature by quantum tunneling or at high temperature by thermal excitation. We show that the requirement that the vacuum survive the high temperatures of the early Universe places the strongest constraints from vacuum stability on the top-quark and Higgs-boson masses in the minimal standard model. If a single Higgs boson is found experimentally, these constraints may place an upper bound on the scale of new physics beyond the minimal standard model. In contrast with other work, we examine temperatures very large compared to the scale of weak symmetry restoration and find much stronger bounds. We also present a simple analytic approximation that directly relates the bounds to the running coupling constants of the minimal standard model.

I. INTRODUCTION

In the minimal standard model, the classical Higgs potential has the form

$$V(\phi)=-\tfrac{1}{2}\mu^2\phi^2+\tfrac{1}{4}\lambda\phi^4 . \tag{1.1}$$

This potential, however, is modified by radiative corrections. As we shall review, the dominant effect of radiative corrections is to replace the couplings μ^2 and λ by running couplings that are evaluated at the scale given by ϕ itself:

$$V_{\rm eff}(\phi)=-\tfrac{1}{2}\mu^2(\phi)\phi^2+\tfrac{1}{4}\lambda(\phi)\phi^4 . \tag{1.2}$$

μ^2 and λ are determined by the Higgs-boson mass at the vacuum expectation value $\sigma=247$ GeV and are then evolved to the scale ϕ using the leading-order β functions:

$$\begin{aligned}\frac{d\lambda}{d(\ln\phi)}&=\beta_\lambda(g(\phi),\lambda(\phi)) ,\\ \frac{d\mu^2}{d(\ln\phi)}&=\mu^2\beta_{\mu^2}(g(\phi),\lambda(\phi)) .\end{aligned} \tag{1.3}$$

Explicit formulas may be found in Ref. [1]. β_λ receives contributions of order λ^2 from scalar loops, g^4 from gauge-boson loops, and a negative contribution of order g_Y^4 from fermion loops. For a top-quark mass large compared to m_H and m_W, the fermion contribution will dominate the others and will drive $\lambda(\phi)$ negative at very large values of ϕ, as depicted in Fig. 1. This destabilizes the effective potential [5], shown qualitatively in Fig. 2, where $\phi_a \ggg \sigma$. The dashed curve in Fig. 3 separates the values of top-quark and Higgs-boson masses for which our vacuum at $\sigma=247$ GeV is absolutely stable and merely metastable. (This figure assumes the minimal standard model is a good effective theory all the way up to the Planck scale, an assumption we shall relax later.) We shall see later that all of the physical scales relevant to false-vacuum decay, the typical ϕ created during nucleation, the size of the nucleation region, and the optimal temperature, are all very roughly the same, so there will be no confusion as to which scale to use for the coupling constants.

The decay of our vacuum occurs by the nucleation of a bubble of the unstable phase. If the bubble is too small, it collapses under its surface tension. If the bubble is large enough, it expands classically, eventually absorbing all of the metastable phase. Figure 4 shows qualitatively the energy of a bubble as a function of its radius when the value of ϕ probed at the center of the bubble is held fixed. (For a more general qualitative discussion, see Ref. [6].) There is an energy barrier inhibiting the formation of sufficiently large bubbles. At zero energy, the vacuum can decay only by quantum tunneling through the barrier, and the rate will be exponentially small [7]. We shall

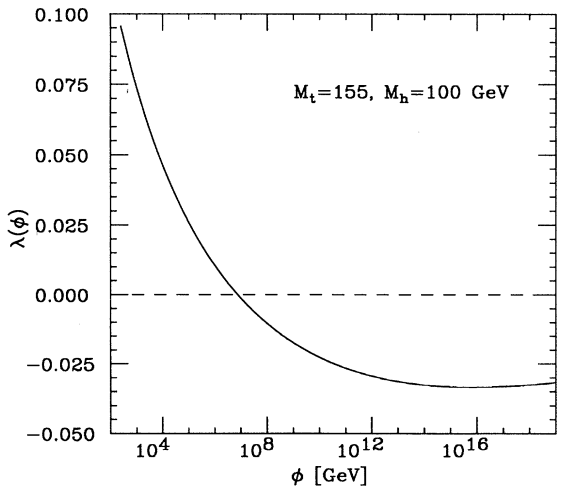

FIG. 1. The running of the scalar self-coupling $\lambda(\phi)$ vs scale ϕ for a sample choice of m_H and m_t which destabilizes the effective potential.

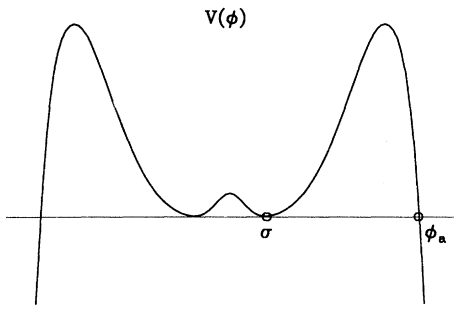

FIG. 2. The effective potential when fermion masses are large enough to destabilize it.

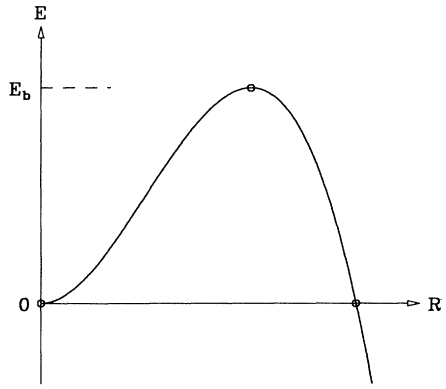

FIG. 4. A qualitative sketch of bubble energy E vs bubble size R for fixed bubble amplitude ϕ_0.

presently review the method for calculating this rate, but the results are shown in Fig. 3. Above the dot-dashed line, the lifetime of our vacuum exceeds the age of the Universe.

If enough energy were present, the energy barrier E_b in Fig. 4 might be crossed classically, rather than quantum mechanically, and so there would be no exponential suppression arising from quantum tunneling. It was once suggested [8] that high-energy cosmic-ray collisions could provide this energy, but one of us [6] argued that such collisions could not produce enough Higgs quanta to create a sufficiently large bubble. Producing such bubbles might be possible if current speculations that weak interactions necessarily become strong at energies of order 10–100 TeV are borne out. The implications for false-vacuum decay have been explored by Ellis, Linde, and Sher [9] and by Hsu [10]. Since this possibility is so highly speculative, its consequences cannot yet be used to exclude any top-quark and Higgs-boson masses.

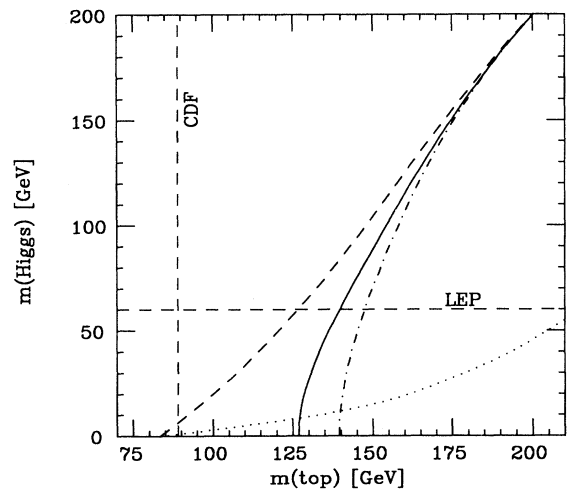

FIG. 3. Below the dashed curve, our vacuum is not absolutely stable. Below the dot-dash curve, it would have already decayed due to quantum tunneling at zero temperature. Below the solid curve, it would have already decayed due to thermal excitation in the early Universe. The dotted line shows the generally weaker bound of Ref. [2] due to thermal excitation below the symmetry-restoration temperature. All curves correspond to a cutoff of $\Lambda=10^{19}$ GeV for the minimal standard model. The current bounds from the CERN e^+e^- collider LEP (Ref. [3]) and the Collider Detector at Fermilab (CDF) (Ref. [4]) are also shown.

Another source of energy to cross the barrier is the high temperature of the early Universe. In the high-temperature plasma, Higgs quanta are as abundant as any other particle, and thermal fluctuations may excite a sufficiently large bubble. That large, coherent, classical excitations may be formed in the thermal plasma has been the subject of some debate and was demonstrated cleanly in the numerical work of Ref. [11]. A qualitative discussion may be found in Ref. [12]. The probability of a thermal fluctuation having sufficient energy E_b to cross the barrier is simply given by a Maxwell-Boltzmann factor $\exp(-\beta E_b)$.

The rate will not be exponentially suppressed at temperatures large compared to the barrier energy. At first sight, this seems to imply that no false vacuum could survive the early history of the Universe. However, the effective potential, and therefore E_b, also depends implicitly on the temperature. We shall review the finite-temperature potential below, but the effect at high temperature is to add a temperature-dependent contribution of order

$$V_{\rm eff}(T)-V_{\rm eff}(T=0)\sim g^2T^2\phi^2 \ . \tag{1.4}$$

This is the usual effect responsible for restoring SU(2) gauge symmetry at high temperatures. This contribution will also raise the potential barrier in Fig. 2 and so will raise the energy E_b needed to initiate vacuum decay in Fig. 4. The advantage of high temperatures to induce vacuum decay hinges on a trade-off: there is thermal energy to cross the barrier, but the barrier is higher. These issues were first addressed by Anderson [2], who restricted his attention to temperatures near or below the symmetry-restoration transition and obtained the bounds shown by the dotted line in Fig. 3. By examining much higher temperatures, we find much stronger bounds on top-quark and Higgs-boson masses, shown by the solid line. We will also show how, to a good approximation, these bounds may be related to the runing coupling con-

stants by a simple analytic formula.

In the next section, we shall briefly review the effective potential. In Sec. III, we discuss the vacuum decay rate at zero temperature and review how the standard model may be excellently approximated by a simple toy model. In Sec. IV, we review the finite-temperature case, explain our calculations, and show how, at high tempertures, the standard model may again be well approximated by a simple extension of our toy model. We also discuss the validity of our approximations and the sources of higher-order corrections.

II. THE EFFECTIVE POTENTIAL

The one-loop correction to the effective potential is, in the Landau gauge [1,13],

$$V_1=\frac{1}{64\pi^2}\left[B\phi^4\ln\frac{\phi^2}{M^2}+(3\lambda\phi^2-\mu^2)^2\ln\frac{3\lambda\phi^2-\mu^2}{M^2}+3(\lambda\phi^2-\mu^2)^2\ln\frac{\lambda\phi^2-\mu^2}{M^2}\right], \tag{2.1}$$

$$B=\tfrac{3}{16}(g_1^4+2g_1^2g_2^2+3g_2^4)-3g_Y^4 , \tag{2.2}$$

where M is the original, fixed renormalization scale, which we shall in practice always choose to be the vacuum expectation value (VEV) σ. In our convention, ϕ represents $|\Phi|/\sqrt{2}$ where Φ is the complex Higgs doublet. At large ϕ, V_1 is dominated by

$$V_1\sim\frac{1}{64\pi^2}(B+12\lambda^2)\phi^4\ln\frac{\phi^2}{M^2} . \tag{2.3}$$

For a sufficiently large top-quark mass, this contribution is negative; at sufficiently large ϕ, it will destabilize the potential. V_1 cannot be trusted at large ϕ, because the two-loop contribution grows as $g^6\ln^2\phi$, the three-loop as $g^8\ln^3\phi$, and so forth. The convergence of the perturbation series is controlled by $g^2\ln\phi$ rather than g^2. When implemented at leading order, the renormalization group implicitly sums the leading-logarithm term in every order and restores convergence; our calculations will be valid to leading order in $g^2(\phi)$ and not merely leading order in $g^2\ln\phi$. The renormalization-group-improved potential is [1,13]

$$V_{\rm RG}(\phi)=-\tfrac{1}{2}\mu^2(\phi)G^2(\phi)\phi^2+\tfrac{1}{4}\lambda(\phi)G^4(\phi)\phi^4 , \tag{2.4}$$

where coupling constants are run numerically using β functions and where each explicit factor of ϕ has been scaled through its anomalous dimension γ using

$$G(\phi)=\exp\left[-\int_M^\phi d(\ln\phi)\gamma(g(\phi))\right] . \tag{2.5}$$

In order to examine processes by which our vacuum may decay, we will need the full effective action rather than just the effective potential. The leading-order Euclidean effective Lagrangian is [13]

$$\mathcal{L}_{\rm eff}=\tfrac{1}{2}G^2(\phi)(\partial\phi)^2-\tfrac{1}{2}\mu^2(\phi)G^2(\phi)\phi^2+\tfrac{1}{4}\lambda(\phi)G^4(\phi)\phi^4 . \tag{2.6}$$

It will be convenient to work with a simply normalized kinetic term. At the order of leading logarithms, and so to leading order in $g^2(\phi)$, we may absorb the wave-function renormalization $G^2(\phi)$ by replacing ϕ by $\phi/G(\phi)$. For the remainder of this work, we shall then work with the effective action

$$\mathcal{L}_{\rm eff}=\tfrac{1}{2}(\partial\phi)^2+V_{\rm eff}(\phi) , \tag{2.7}$$

$$V_{\rm eff}=-\tfrac{1}{2}\mu^2(\phi)\phi^2+\tfrac{1}{4}\lambda(\phi)\phi^4 . \tag{2.8}$$

The prescription is trivial: just evaluate the coupling constants at scale ϕ.

In general, the question of whether or not the electroweak vacuum is necessarily unstable will depend on the scale Λ at which new physics comes in beyond the minimal standard model. The most conservative assumption, for the sake of setting bounds on top-quark and Higgs-boson masses, is to assume the vacuum unstable only if $V_{\rm eff}(\phi)$ drops below $V_{\rm eff}(\sigma)$ for $\phi\lesssim\Lambda$. Figure 5 shows how the unstable region of parameter space varies with Λ. This has been computed more accurately by previous authors, who include next-to-leading-order corrections to the effective potential [14].

At ϕ near or below the vacuum expectation value σ, the effective potential (2.8) does not exactly reproduce the one-loop potential (2.1). This is because it ignores the scalar threshold and treats $\ln(a\lambda\phi^2-\mu^2)$ as $\ln\phi$. The dominant mechanism for vacuum decay, however, will always involve ϕ large compared to σ. Near σ, in any case, the discrepancy is subleading order in $\lambda(\phi)$. For ϕ much smaller than σ, we could remove the scalar contribution to the β function, but this is not really necessary since λ will generally be small. Regardless, the details of the behavior at very small ϕ will not be relevant for our final results. We also cut off numerical evolution of the couplings below 1 GeV in order to avoid the blow-up of α_s. (α_s affects the running of λ and μ^2 indirectly by affecting

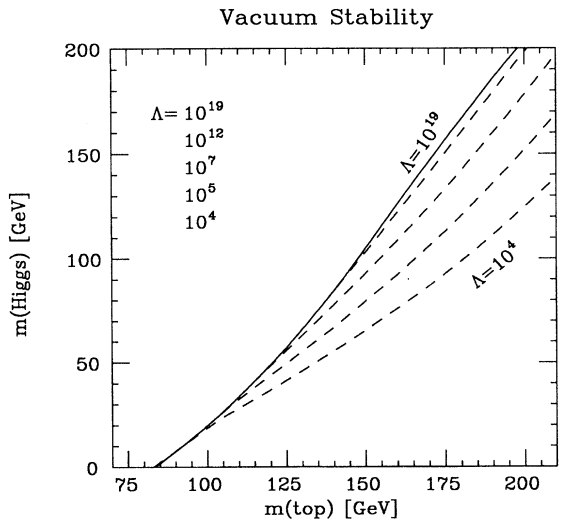

FIG. 5. The line separating a stable electroweak vacuum from one that is merely metastable, as a function of the cutoff scale Λ in GeV.

the running of the top-quark Yukawa g_Y.) Our choice of α_s at the scale $\sigma=247$ GeV is 0.100. [Our initial value of $\alpha_s(\sigma)$ corresponds to $\Lambda_{\rm QCD}$ (4 flavors) $=260$ MeV for the two-loop modified minimal subtraction scheme ($\overline{\rm MS}$) value (ignoring the top quark). But we have simply used *first*-order β-functions to evolve to higher scales since our calculation does not consistently include next-to-leading-order effects in α_s. The evolution above σ includes the top quark and so assumes six flavors. Lowering $\Lambda_{\rm QCD}$ to 100 MeV gives an initial $\alpha_s(\sigma)=0.088$ and decreases our final bounds on m_t by up to 5 GeV.]

III. NUCLEATION BY QUANTUM TUNNELING

The WKB amplitude for false-vacuum decay by tunneling may be found by formally examining the Euclidean path integral and expanding it about the "bounce" solution to the Euclidean equations of motion [15]:

$$\partial^2\phi=\frac{dV_{\rm eff}}{d\phi} . \tag{3.1}$$

The bounce solution is an O(4) rotationally symmetric solution and so solves

$$\left[\partial_s^2+\frac{3}{s}\partial_s\right]\phi=\frac{dV_{\rm eff}}{d\phi} , \tag{3.2}$$

where $s=(t_E^2+\mathbf{r}^2)^{1/2}$. There is a solution which takes on some value ϕ_0 at $s=0$, probing the unstable region of the potential, and which falls to the false vacuum σ as $s\to\infty$. When viewed as a function of Euclidean time t_E, the bounce solution $\phi(s)$ interpolates between the false vacuum $\phi(t_E\to-\infty,\mathbf{r})=\sigma$ and a zero-energy bubble $\phi(t_E=0,\mathbf{r})$, which is large enough to then expand on its own classically. The full Euclidean bounce solution double counts the transition by returning back to the false vacuum $\phi(t_E\to+\infty,\mathbf{r})=\sigma$. The Euclidean action of the solution yields the exponential suppression of the rate for false-vacuum decay:

$$\text{rate}\sim\exp(-S_E) . \tag{3.3}$$

The prefactors of the exponential, if desired, may be computed by an appropriate expansion of the Euclidean path integral about the bounce solution.

At this point, the rate for the decay of the electroweak vacuum at zero energy may be found simply by solving (3.2) numerically, using the effective potential discussed earlier, and computing the Euclidean action. However, as discussed in Ref. [6], there is also a simple but accurate approximation to $V_{\rm eff}$ which produces an analytic result for the bounce solution. The effective potential does not generally become unstable until ϕ is exponentially large compared to σ. For such large ϕ, the quadratic ϕ^2 term may be ignored compared to the quartic ϕ^4 term. In the unstable region, $\lambda(\phi)$ varies only logarithmically with ϕ and so, in first approximation, may be treated as a negative constant ($-\kappa$) over any given decade in ϕ. This inspires the toy model defined by

$$V(\phi)=-\tfrac{1}{4}\kappa\phi^4 . \tag{3.4}$$

The false vacuum at $\phi=0$ is classically stable against all small, *local* perturbations because of the contribution of the gradient term $\frac{1}{2}(\nabla\phi)^2$ to the energy density, which is responsible for the "surface" energy of small bubbles of $\phi\neq0$. The Euclidean bounce solution is the Fubini instanton [16]

$$\phi(s)=\left[\frac{2}{\kappa}\right]^{1/2}\frac{2R}{s^2+R^2},\quad S_E=\frac{8\pi^2}{3\kappa} . \tag{3.5}$$

The solution is degenerate with respect to the choice of an arbitrary scale length R, reflecting the scale invariance of the potential (3.4). In the real standard model, however, this scale invariance is broken by the runing of λ, and R should be chosen to maximize the tunneling rate. (We continue to ignore the mass term, which also breaks scale invariance.) So

$$S_E\approx\frac{8\pi^2}{3\kappa_{\rm eff}},\quad \kappa_{\rm eff}=\max[-\lambda(\phi)]>0 , \tag{3.6}$$

where the maximum is restricted to scales ϕ below the cutoff scale Λ. This approximation generally matches the full numerical calculation of the bounce action to within a few percent.

The rate for false-vacuum decay per unit volume has dimensions of [mass^4]. Since the only mass scale in the toy-model problem is $1/R$, which is the same as $\phi^4(0)$ up to powers of the coupling constant, the approximation (3.6) used to obtain the rate may be slightly improved by writing

$$\frac{\Gamma}{V}\approx\max_{\lambda(\phi)<0}[\phi^4\exp(-S_E)] . \tag{3.7}$$

A more accurate calculation of the prefactor would require expanding the Euclidean path integral in small fluc-

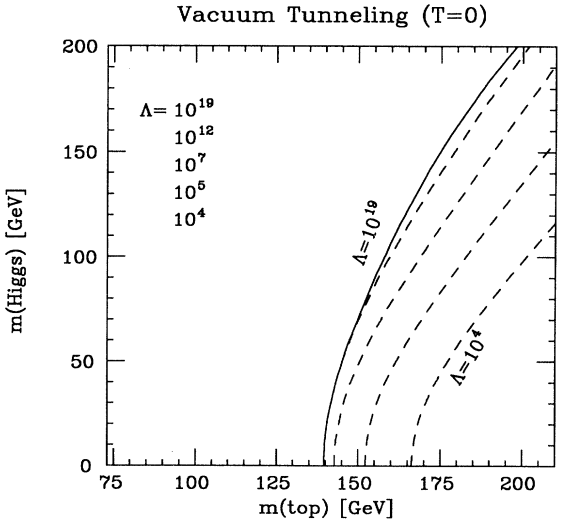

FIG. 6. For various choices of the scale Λ for new physics beyond the minimal standard model, the region below the corresponding line is excluded because our vacuum would have already decayed by quantum tunneling at zero temperature.

tuations about the bounce solution, which we shall not attempt. To decide whether the vacuum would survive 10^{10} yr, we must multiply by the space-time volume of the past light cone of the observable Universe, which is roughly e^{409}/σ^4. The dividing dot-dash line in Fig. 3 is then determined by the criteria that

$$e^{409} \max_{\lambda(\phi)<0} \left[\left[\frac{\phi}{\sigma} \right]^4 \exp\left[-\frac{8\pi^2}{3|\lambda(\phi)|} \right] \right] \sim 1 \ . \tag{3.8}$$

Figure 6 shows how this line depends on the cutoff scale Λ.

IV. NUCLEATION BY THERMAL EXCITATION

At finite temperature, the one-loop potential should be evaluated using finite-temperature Feynman rules. For each species of particle that runs around the loop, the contribution of a nonzero temperature to the effective potential is simply the free energy of an ideal gas of such particles [1,17]:

$$V_{\rm eff}(T,\phi) = V_{\rm eff}(0,\phi) + \sum_i \pm n_i T \int_0^\infty \frac{d^3k}{(2\pi)^3} \ln\{1 \mp \exp[-\beta\sqrt{k^2+m_i^2(\phi)}]\} \ , \tag{4.1}$$

where the sum is over all species i, n_i is the number of degrees of freedom associated with each species, the upper (lower) sign is for bosons (fermions), and $m_i(\phi)$ is the effective mass of species i in the presence of ϕ. For example,

$$m_W(\phi) = \tfrac{1}{2} g_2 \phi, \quad n_W = 6 \ ,$$
$$m_Z(\phi) = \tfrac{1}{2}(g_1^2+g_2^2)^{1/2}\phi, \quad n_Z = 3 \ ,$$
$$m_t(\phi) = g_Y \phi/\sqrt{2}, \quad n_t = 12 \ . \tag{4.2}$$

The details of the scalar contributions, however, are gauge dependent. The gauge dependence disappears in the high-temperature limit, where [17,18]

$$V_{\rm eff}(T,\phi) \approx V_{\rm eff}(0,\phi) + \tfrac{1}{2} g^2 T^2 \phi^2 + \text{const} \ , \tag{4.3}$$
$$g^2 \equiv \tfrac{1}{12}(\tfrac{3}{4}g_1^2 + \tfrac{9}{4}g_2^2 + 3g_Y^2 + 6\lambda) \ . \tag{4.4}$$

We shall see later that, for processes which thermally excite the phase transition, either the high-temperature limit is valid or else λ is order g^4 and the gauge-dependent scalar effects are ignorable. In fact, for the bounds on the top-quark and Higgs-boson mass, the high-temperature limit will always be adequate. For more general numerical work, we shall take the finite-temperature corrections to $V_{\rm eff}$ to be given by (4.1) with the scalar contribution replaced by its high-temperature limit:

$$V_{\rm eff}(T,\phi) \approx V_{\rm eff}(0,\phi) + \tfrac{1}{4}\lambda T^2\phi^2 + \sum_{i=W,Z,t} \pm n_i T \int_0^\infty \frac{d^3k}{(2\pi)^3} \ln\{1 \mp \exp[-\beta\sqrt{k^2+m_i^2(\phi)}]\} \ . \tag{4.5}$$

We shall evaluate coupling constants at the scale ϕ as before. As we shall see below, the optimal temperature for thermally exciting phase transitions is roughly the same order as the ϕ probed in the nucleation process, and so there will be no serious ambiguity associated with which scale to use for coupling constants.

The location of the false vacuum of $V_{\rm eff}$ is temperature dependent. At low temperature, it is at σ; at high temperature it is at zero. Using the effective potential of (4.5) and (2.8), the phase transition is first order, as shown in Fig. 7. However, the dominant contribution to false-vacuum decay will be at sufficiently high temperature that it will be insensitive to the possibly complicated details of the phase transition.

We now need to find the energy barrier for the phase transition, corresponding to E_b in Fig. 4. Note that the bubble corresponding to E_b is a static, unstable solution to the classical equations of motion: a bubble unstably balanced between expansion and collapse. This bubble may be found by solving the static equations of motion [19]:

$$\nabla^2\phi = \frac{dV_{\rm eff}}{d\phi} \ .$$

Making a spherical ansatz, this becomes

$$\left[\partial_r^2 + \frac{2}{r}\partial_r \right] \phi = \frac{dV_{\rm eff}}{d\phi} \ .$$

We are now in a position to find the thermal decay rate $\exp(-\beta E_b)$ of the vacuum by solving this equation numerically and computing the solution's energy E_b. Again, we search for a solution that probes unstable values of ϕ at $r=0$ and falls off to the appropriate (temperature-dependent) vacuum as $r \to \infty$.

Figure 8 gives an example of the dependence of the exponent $\beta E_b(T)$ for a particular choice of top-quark and Higgs-boson mass. Anderson [2], who was the first to

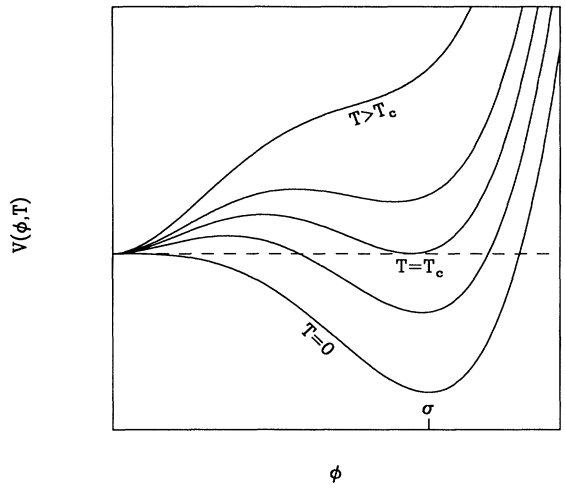

FIG. 7. A qualitative picture of the effective potential as a function of ϕ for various temperatures covering the phase transition at T_c. This figure shows only the behavior near and below σ; for large m_t, there will also be the instability of $V(\phi)$ at very large ϕ as in Fig. 2. Except at low values of m_H, the phase transition is much weaker than depicted here.

look seriously at thermal excitation of false-vacuum decay in this context, examined the process at temperatures below the symmetry-restoration temperature T_c. He found the corresponding local minimum of βE and used it to estimate the maximal decay rate due to thermal excitation. His bounds on the top-quark and Higgs-boson mass are shown by the dotted line in Fig. 3. However, Fig. 8 shows that the rate is much greater at temperatures very large compared to T_c. The resulting bounds on masses are generally much stronger. The discontinuous jump in Fig. 8 at T_c is due to the discontinuous change in the vacuum state in a first-order phase transition.

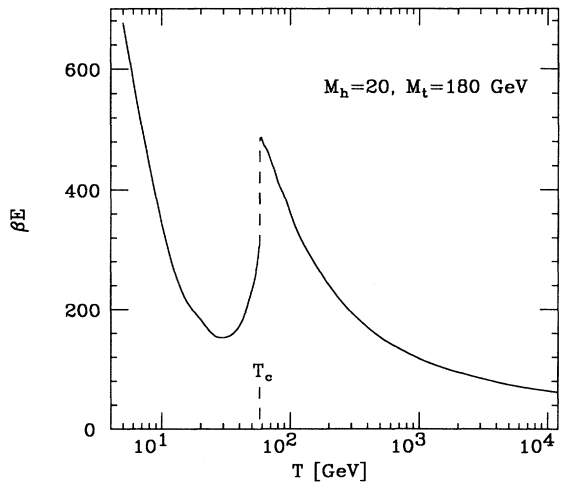

FIG. 8. The Maxwell-Boltzmann exponent $\beta E(T)$ as a function of temperature for a particular choice of m_H and m_t. The numerical discrepancy below T_c with Fig. 3 of Ref. [2] is due to the sensitivity of the maximum of $V_{\rm eff}$ to the Higgs-boson mass. The resulting bounds on m_H and m_t, however, are relatively insensitive.

As before, there is a simple approximation to $V_{\rm eff}$ which produces a simple equation for E_b. Let us again approximate the zero-energy effective potential by $-\frac{1}{4}\kappa\phi^4$, and now approximate the finite-temperature contribution by its high-temperature limit

$$V(\phi)=\tfrac{1}{2}g^2T^2\phi^2-\tfrac{1}{4}\kappa\phi^4 .$$

Now scale out masses and coupling constants by replacing

$$\phi\to gT\bar{\phi}/\sqrt{\kappa},\quad r\to\bar{r}/(gT) . \tag{4.6}$$

The energy functional then becomes

$$E=\frac{gT}{\kappa}\int d^3\bar{r}\left[\tfrac{1}{2}(\nabla\bar{\phi})^2+\tfrac{1}{2}\bar{\phi}^2-\tfrac{1}{4}\bar{\phi}^4\right] , \tag{4.7}$$

and so E_b is proportional to gT/κ. The constant of proportionality may be found by solving the equations of motion numerically:

$$\left[\partial_{\bar{r}}^2+\frac{2}{\bar{r}}\partial_{\bar{r}}\right]\bar{\phi}=\bar{\phi}-\bar{\phi}^3 ,$$

giving [20]

$$\beta E_b=(6.015)\pi g/\kappa . \tag{4.8}$$

From (4.6), the size of the bubble is order $1/gT$ and the typical ϕ is order $gT/\sqrt{\kappa}$. In this toy model, the exponent βE_b is independent of the temperature T.

In the real standard model, this independence of scale will again be broken by the running of couplings, and we should look for the temperature that minimizes $g(T)/|\lambda(T)|$ when $\lambda(T)$ is negative. As before, we have essentially one scale in the problem, and the rate per unit volume will be roughly $T^4\exp(-\beta E_b)$. As discussed by Anderson, we should now multiply by the volume our current horizon had when at temperature T, which is

$$V(T)\sim(10^{10}\ {\rm yr})^3\times(3{\rm K}/T)^3 , \tag{4.9}$$

and by the amount of time the Universe spent at temperature T, which is

$$t\sim M_{\rm pl}/T^2 . \tag{4.10}$$

Putting it together, the solid line in Fig. 3 is then determined by the condition

$$e^{232}\max_{\lambda(T)<0}\left[\left[\frac{\sigma}{T}\right]\exp\left[-\frac{6.0\pi g(T)}{|\lambda(T)|}\right]\right]\sim 1 , \tag{4.11}$$

where $g(T)$ is given by (4.4) and the maximum is restricted to scales $T\le\Lambda$. Note that, if coupling constants are sufficiently small, the exponent of order $g/|\lambda|$ for thermal excitation should always beat the exponent of order $1/|\lambda|$ for tunneling at zero temperature. Indeed, our numerical results bear out this conclusion.

Figure 9 shows the dependence of the bounds on the scale Λ for physics beyond the minimal standard model. Anderson's results for processes below the symmetry-

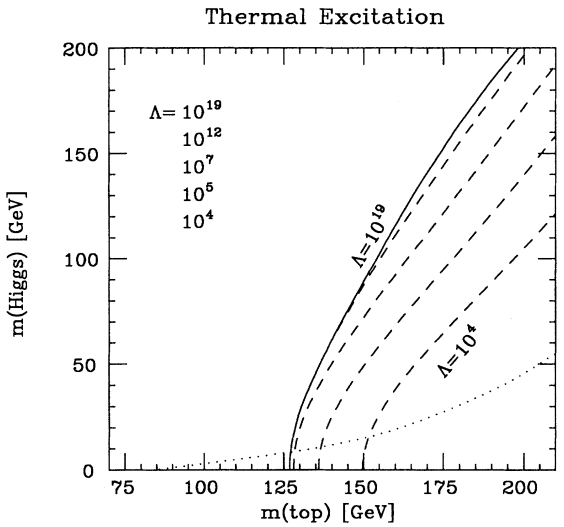

FIG. 9. As in Fig. 6, but for decay of the false vacuum by thermal excitation at high temperature. The dotted line is the bound of Ref. [2] from processes below the temperature of symmetry restoration. The total bound from thermal excitation is the union of the dotted curve with the appropriate high-temperature curve.

restoration temperature T_c are again shown by the dotted line. Consider again the behavior of the Maxwell-Boltzmann exponent βE depicted in Fig. 8. At very low m_H, βE for $T > T_c$ never drops below the local minimum for $T < T_c$. In this case, Anderson's bound beats the high-temperature bound, as shown in Fig. 9.

We are now in a position to check under what conditions the high-temperature limit needed to justify our toy model is a good one. This limit of the effective potential (4.1) is valid when T is large compared to the particle masses $m_i(\phi) \sim g\phi$. In our solution, $g\phi \sim g^2 T/\sqrt{|\lambda|}$ by (4.6), and so the high-temperature limit is valid if $\lambda \gg g^4$.

The best test of the approximation is simply to compare the mass bounds to those derived using the full potential of Eqs. (2.8) and (4.5), solving numerically for the static solutions. This is computationally expensive, and so we have only checked a few representative values. The approximation for the $\Lambda = 10^{19}$ GeV curve is valid to within a few GeV in m_t. The approximation gets worse at small Λ, and the exact definition of Λ itself becomes crucial, as seen by the variation of the curves in Fig. 9 with Λ. Physically, the scale Λ of new physics is not a precisely defined quantity, and only its order of magnitude is relevant. For the purposes of testing our approximation, however, let us define it by considering only temperatures where the solution for the energy barrier has $\phi(0) \leq \Lambda$. (Such solutions also have $T < \Lambda$ and $1/R < \Lambda$.) The $\Lambda = 10^4$ curve is then valid to about ± 5 GeV in m_t. This is likely the same size as corrections due to next-to-leading-order effects, which have not been included [14].

Is it worth computing the curves of Fig. 9 more accurately, by both using exact numerical solutions and by including next-to-leading-order effects? Since the precise value of Λ is not physically meaningful, the curves in Fig. 9 are intrinsically fuzzy by variations of Λ by roughly an order of magnitude. Corrections to the curves will not be meaningful unless they exceed this variation. The most important application for corrections is then for the case of very large Λ, where the variation is small. Next-to-leading-order effects would include corrections to the β functions, corrections to the finite-temperature potential, and the full computation of small fluctuations about the bubble solution $\phi(r)$. Other issues that must be addressed at higher order are the gauge dependence of the effective potential and the fact that it can be complex valued. We are currently investigating the calculation of these next-to-leading-order corrections.

We should mention one correction whose smallness may not be obvious. At finite temperature, particles have thermal masses of order gT (related to Debye screening) which may be of the same order as their ϕ-dependent mass of $g\phi$. Such a contribution should be included in the computation of the effective potential (4.1) [21]. In the high-temperature limit, valid when $|\lambda| \gg g^4$, the thermal contribution to the total mass just adds an uninteresting constant to the effective potential and may safely be ignored at leading order. If, on the other hand, $|\lambda| \sim g^4$, then our bubble has $\phi \sim gT/\sqrt{|\lambda|} \sim T/g$ and the ratio of the thermal mass to the ϕ-dependent one is $(gT)/(g\phi) \sim g$. The thermal mass can again be ignored at leading order.

V. CONCLUSIONS

We have shown that the strongest bounds on the stability of the electroweak vacuum come from decays induced by thermal excitation in the early Universe. These bounds are sensitive to the scale Λ up to which the minimal standard model and the standard big-bang scenario may be good effective theories of nature. If the top quark and a Higgs candidate are found in a region that is excluded when Λ is the Planck scale, then Fig. 9 can be used to read off an upper bound on the scale Λ of new physics beyond either the minimal standard model or the standard big bang. If the masses are also in a region excluded by the zero-temperature limits of Fig. 6, then a weaker upper bound on the scale of Λ can be read off that is independent of the big-bang scenario. Finally, there is the intriguing possibility that we may someday discover that the minimal standard model is a good effective theory up to 10 TeV or so and discover masses in a region where our vacuum is metastable for $\Lambda \geq 10$ TeV. We would then know our vacuum will someday decay, billions of year hence.

ACKNOWLEDGMENT

This work was supported by the U.S. Department of Energy, Division of High Energy Physics, Contract No. W-31-109-ENG-38.

[1] For a review of the electroweak Higgs potential, see M. Sher, Phys. Rep. **179**, 274 (1989).
[2] G. Anderson, Phys. Lett. B **243**, 265 (1990).
[3] ALEPH Collaboration, D. Decamp *et al.*, Phys. Lett. B **262**, 139 (1991).
[4] K. Sliwa, in *High Energy Hadronic Interactions,* Proceedings of the XXVth Rencontres de Moriond, Les Arcs, France, 1990, edited by J. Tran Thanh Van (Editions Frontières, Gif-sur-Yvette, 1990).
[5] H. D. Politzer and S. Wolfram, Phys. Lett. **82B**, 242 (1979); P. Q. Hung, Phys. Rev. Lett. **42**, 873 (1979); N. Cabibbo, L. Maiani, A. Parisi, and R. Petronzio, Nucl. Phys. **B158**, 295 (1979).
[6] P. Arnold, Phys. Rev. D **40**, 613 (1989).
[7] R. Flores and M. Sher, Phys. Rev. D **27**, 1679 (1982); M. Duncan, R. Philippe, and M. Sher, Phys. Lett. **153B**, 165 (1985); Phys. Lett. B **209**, 543(E) (1988).
[8] M. Sher and H. Zaglauer, Phys. Lett. B **206**, 527 (1988).
[9] J. Ellis, A. Linde, and M. Sher, Phys. Lett. B **252**, 203 (1990).
[10] S. Hsu, Phys. Lett. B **261**, 81 (1991).
[11] D. Grigoriev, V. Rubakov, and M. Shaposhnikov, Phys. Lett. B **216**, 172 (1989); Nucl. Phys. **B191**, 382 (1990); D. Grigoriev and V. Rubakov, *ibid.* **B299**, 67 (1988).
[12] M. Dine, O. Lechtenfeld, and B. Sakita, Nucl. Phys. **B342**, 381 (1990).
[13] S. Coleman and E. Weinberg, Phys. Rev. D **7**, 1888 (1973).
[14] M. Lindner, M. Sher, and H. Zaglauer, Phys. Lett B **288**, 139 (1989).
[15] For a review on the application of semiclassical techniques to tunneling problems in field theory, see S. Coleman, in *The Whys of Subnuclear Physics,* Proceedings of the International School of Subnuclear Physics, Erice, Italy, 1977, edited by A. Zichichi, Subnuclear Series Vol. 15 (Plenum, New York, 1979), p. 805.
[16] S. Fubini, Nuovo Cimento A **34**, 421 (1976).
[17] L. Dolan and R. Jackiw, Phys. Rev. D **9**, 3320 (1974).
[18] S. Weinberg, Phys. Rev. D **9**, 3357 (1974).
[19] A. Linde, Phys. Lett. **70B**, 206 (1977); **100B**, 37 (1981); A. Guth and E. Weinberg, Phys. Rev. D **23**, 876 (1981).
[20] E. Brezin and G. Parisi, J. Stat. Phys. **19**, 269 (1978).
[21] P. Fendley, Phys. Lett. B **196**, 175 (1987).